FAST DYNAMIC MAGNETIC RESONANCE IMAGING USING TAGGING RF PULSES

Vimal Singh *Ahmed H. Tewfik*

The University of Texas at Austin, Texas, USA

ABSTRACT

A critical requirement for dynamic magnetic resonance imaging (MRI) is to reduce image acquisition times while maintaining high spatial resolutions to capture the underlying process with high-information rates. This paper presents a sparse signal recovery based fast MRI method which uses: 1) dictionary learning for sparse representation of signals for encoding of data redundancy in physiological functions and, 2) a tagging radio-frequency pulses based novel MR signal encoding formulation to uniformly sample the k-space, even at high acceleration factors. The preliminary results of dynamic MR image recovery experiments using tagging based MR signal acquisition method on an in-vivo myocardial perfusion dataset outperforms the equivalent dynamic MRI method implemented with variable density k-space under-sampling.

Index Terms— Sparse Representations, MR Signal Encoding, Tagging Pulses, Dynamic MRI, Dictionary Learning

1. INTRODUCTION

Diagnosis of various heart-related abnormalities relies on magnetic resonance imaging (MRI) of the cardiovascular functions. For example, first-pass myocardial perfusion MRI is used to detect and evaluate ischemic heart disease [1]. A critical requirement for functional cardiac MRI is to reduce image acquisition times while maintaining high spatial resolutions to capture the underlying process with high-information rates. Due to physical and physiological constraints data acquisition in MRI is sequential in time. Consequently, due to limited acquisition time in dynamic MRI, the recovered images have low signal-to-noise ratios and/or poor resolutions. Previously, many techniques based on exploiting the raw data redundancy in the spatial and/or the temporal dimensions have been presented to reduce the acquisition time for dynamic MRI [2, 3]. These techniques have shown limited performance improvements at low accelerations. More recently, many fast structural MRI techniques based on the theory of Compressed Sensing (CS) have emerged [4]. CS based MRI methods rely on recovering the sparse representation of the underlying image in a sparsifying basis which exhibits high incoherency with the sensing basis. In MRI, spatial-Fourier (multi-dimensional) is the standard sensing basis and is also commonly known as the k-space. In an attempt to improve the incoherency between the sparsifying and sensing bases, few techniques have proposed on modifying the MR signal encoding formulation i.e., the sensing basis. In this paper, a fast dynamic MRI method based on spatio-temporal redundancy encoding within a sparse signal recovery framework along with a non-Fourier MR signal encoding is presented.

Recently, fast dynamic MRI techniques exploiting the inherent redundancy of the physiological functions within the sparse signal recovery formulations have emerged [5, 6, 7]. The highly constrained back projection (HYPR) method of [5] relies on sharing of high frequency details between individual time frames of an image time-series and oversampling the contrast information for each time-frame to recover sparse MR angiographic images at high acceleration factors ~ 100. However, for not-so-sparse myocardial perfusion images, acceleration gains of 4 only, have been reported [6]. In [7], authors separate the redundancy encoding for low- and high-frequency regions of the k-space into spatial-Fourier and image-patch space, respectively. Redundancy encoding corresponds to learning multiple dictionaries for sparse representation of the corresponding regions of k-space in the appropriate transform domain. The MR image is recovered through sequential recovery of sparse representations of the low- and high-frequency regions in the learned dictionaries. Aforementioned techniques use the spatial-Fourier transform based MR signal encoding formulation, which limits their performance at high accelerations. At high accelerations, image details are lost either due to sharing of mutually exclusive information over long temporal windows [6] or due to the lack of adequately sampled high frequency information needed to drive the recovery of sparse representation of peripheral region of the k-space [7].

This paper presents a fast dynamic MRI method using a novel MR signal encoding formulation. The proposed dynamic MRI method like [7] uses dictionary learning for sparse representation of image-patches for redundancy encoding but uses a new MR signal encoding formulation based on spatial modulations by using tagging radio frequency (RF) pulses for raw data acquisition. Tagging RF pulses are used clinically in cardiovascular MRI for evaluation of regional myocardial functions [8, 9]. The new signal encoding formulation varies the spatial weights for each MR excitation within the imaging slice using tagging pulses. Specifically, the spatial magnitude modulation (SPAMM) pulse sequences are proposed to be used to generate the spatial weights [8]. The proposed formulation is inspired from the randomized encoding formulation of [10] which uses tailored spatially-selective RF pulses to obtain Gaussian randomized spatial modulations. A limiting factor for the randomized encoding formulation is their accurate realization on the physical hardware, due to which the theoretical formulation differs from the realized formulation and leads to errors [10]. Motivated by the limitations of the randomized formulation, the tagging RF pulses based encoding formulation is proposed. Since, the new formulation uses clinically active SPAMM RF pulses its hardware realization will be closer to its theoretical modeling than that for the randomized formulation of [10].

The true innovation of the proposed fast dynamic MRI method is the synergistic combination of image-details based redundancy encoding with the tagging based MR signal encoding formulation. The modulation of spatial amplitudes in the proposed signal encoding formulation leads to acquisition of raw data samples which are mixtures of the standard k-space samples. Thus, the new formulation leads to a more uniform coverage of k-space information even at high accelerations unlike the variable density under-sampled Fourier encoding previously used in [6, 7]. The preliminary results of dynamic MRI recovery experiments on an in-vivo myocardial perfusion dataset show that the proposed approach with tagging based MR signal acquisition preserves details like edges and fine structures in recovered images better than when the variable density based k-space signal acquisition is used.

The rest of this paper is organized as follows. Section 2 presents a mathematical treatment of the complete fast dynamic MRI method. Section 3 summarizes the simulation experiment results on the in-vivo myocardial perfusion dataset. Finally, section 4 concludes the paper.

2. METHOD

This section presents a mathematical formulation of the proposed dynamic MR imaging technique. Section 2.1 presents the proposed tagging pulses based MR signal encoding formulation along with a short review of the SPAMM sequences. In section 2.2, the redundancy encoding formulation using dictionary learning technique for image details is presented. Finally, the image recovery problem is formulated and details on the algorithm used are provided in section 2.3.

2.1. Encoding using MR Tagging Pulses

The MR signal acquisition equation for a single excitation is

$$d(k_m) = \int w_m\,(r)\,\rho\,(r)\exp\left(-i2\pi k_m.r\right)dr \tag{1}$$

where, $d(k_m)$ is the m^{th} MR sample trajectory, $\rho\,(r)$ is the desired image, k_m is a time-integral function of field gradients employed and w_m is a weighting factor. In clinical MR, w_m remains constant for all excitations of the image acquisition procedure and can account for spatial modulations either due to the fixed spatial sensitivity of a surface coil or the spatial magnetization modulation (SPAMM) obtained using tagging pulses. An assumption for the latter case is that the fading of the SPAMM is negligible during the readout time, i.e., in clinical MR, $w_m(r)$ is not a function of m.

2.1.1. Spatial Magnitude Modulation

The basic tagging pulse sequences rely on perturbing the longitudinal magnetization prior to the imaging stage such that visible markers are created [9]. The SPAMM pulses wrap the magnetization in a sinusoidal fashion through space by applying two equal-strength non-selective RF pulses separated by a 'wrapping' gradient [8, 9]. The spatial magnetic modulation can be represented as

$$w_m(r) = \left|\cos\frac{2\pi}{T_m}\;r.v_m\right| \tag{2}$$

where, T_m is the period of the modulation, v_m is the vector gradient field applied during the tagging phase and $|.|$ is the absolute value operator. The magnitude of v_m controls the period of the sinusoidal modulation and its direction identifies the axis of signal modulation. For obtaining a gridded-tag pattern two SPAMM tagging phases with perpendicular v_m directions are used [9].

In the proposed MR signal encoding formulation the weight factor w_m will be varied from excitation to excitation and this weighting will be achieved using the tagging RF pulses as described by (2). Intuitively, the spatial modulation of magnetization leads to convolution in the spatial-Fourier domain (k-space). Thus, in the new encoding formulation MR samples are a mixture of the standard k-space samples. Towards this end, the following MR signal encoding framework is proposed:

$$d(k_m) = \int w_m\,(r)\,\rho\,(r)\exp\left(-i2\pi k_{(m,x)}x\right)dx \tag{3}$$

Ideally, the spatial modulation $w_m(r)$ in (3) can be obtained through concatenation of multiple tagging phases before the imaging phase. However, for practical purposes and for all results presented in this paper, concatenation of two tagging phases is proposed. This allows for efficient realization of SPAMM pulse sequences and leads to mixing along multiple dimensions of the k-space. Now, a discretization of (3) can be represented as:

$$d_{TE,i} = \mathcal{F}_{1d}\;\mathbf{W}_{TE,i}\;\rho \tag{4}$$

where, $d_{TE,i}$ are the tag encoded samples of the i^{th} excitation, $\mathcal{F}_{1d}$ is the 1-dimensional Fourier transform matrix, $\mathbf{W}_{TE,i}$ is the discrete spatial modulation and ρ is the voxel-image. Now, extending the equation (4) to M excitations, the complete tagging based MR encoding formulation can be represented as:

$$\begin{aligned} d_{TE} &= \begin{bmatrix} \mathcal{F}_{1d} & \mathbf{0} & \dots & \mathbf{0} \\ \mathbf{0} & \mathcal{F}_{1d} & \dots & \mathbf{0} \\ \vdots & \vdots & \ddots & \vdots \\ \mathbf{0} & \mathbf{0} & \dots & \mathcal{F}_{1d} \end{bmatrix} \begin{bmatrix} \mathbf{W}_{TE,1} \\ \mathbf{W}_{TE,2} \\ \vdots \\ \mathbf{W}_{TE,M} \end{bmatrix} \rho && \text{(5a)} \\ &= \mathbf{E}\;\rho && \text{(5b)} \end{aligned}$$

where, d_{TE} are all the acquired tag encoded samples, E represents the encoding matrix and $\{W_{TE,i}\}_{i=1}^{M}$ are the M spatial modulations employed.

2.2. Redundancy Encoding

As stated earlier, the proposed dynamic imaging method relies on dictionary learning for sparse representation of image-details as the redundancy encoding formulation. Furthermore, since image details such as edges and fine structures are localized in image-space, a dictionary for sparse representation of image-patches is proposed. To learn a patch-based dictionary from a given image ρ, the following problem is solved:

$$\min_{\mathbf{G},\Gamma}\;\sum_j \parallel \mathbf{G}\alpha_j - R_j\rho \parallel_2^2\;\; s.t.\;\parallel \alpha_j \parallel_0\;\leq\;T_0\;\;\forall\, j \tag{6}$$

where, R_j is a patch extraction operator, the l_0 quasi-norm encodes the sparsity of representation and T_0 is the degree of sparsity. Γ is used to denote the set $\{\alpha_j\}_j$ of sparse representation of all patches and $\mathbf{G}$ is the patch-based dictionary. The formulation of (6), minimizes the total fitting error of all image patches with respect to the dictionary $\mathbf{G}$, subject to sparsity constraints. For all results reported in this paper, the K-SVD algorithm of [11] has been used to learn the patch-based dictionary $\mathbf{G}$. The K-SVD is an two-step iterative technique which alternates between a sparse coding and a dictionary-atom update step to learn a dictionary for sparse representation of training data[11]. The reference images for training the dictionary $\mathbf{G}$ can be few fully spatial-Fourier encoded image planes which can be acquired in a rest-phase prior to the dynamic imaging procedure.

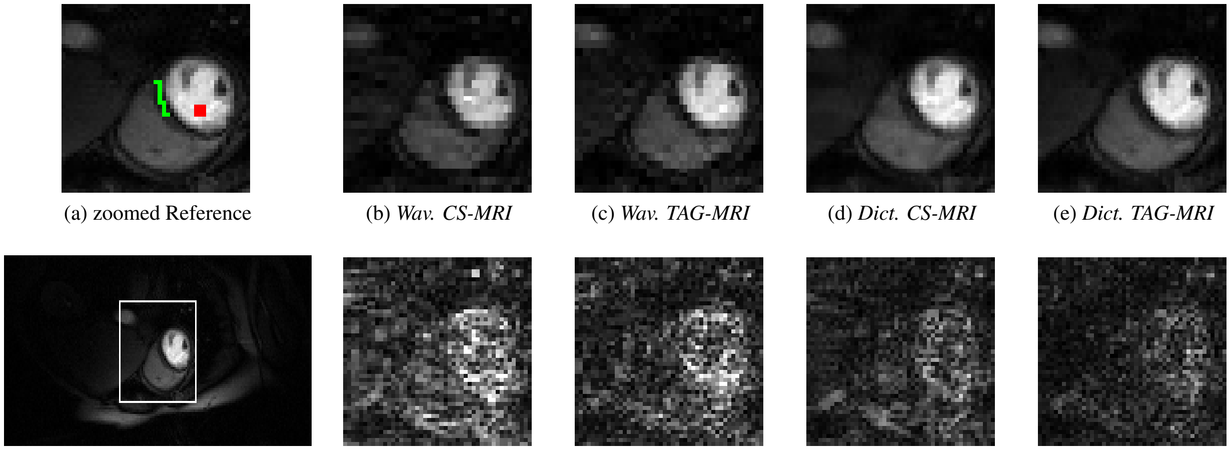

(a) zoomed Reference (b) *Wav. CS-MRI* (c) *Wav. TAG-MRI* (d) *Dict. CS-MRI* (e) *Dict. TAG-MRI*

(f) Reference (g) (0.297, 0.8520) (h) (0.284, 0.8508) (i) (0.197, 0.9023)) (j) (0.184, 0.9132)

Fig. 1: Comparison of image recovery for four different MR image recovery techniques as described in section 3 at acceleration R = 4. (a) shows a zoomed-in region of the reference image (f). For all other columns, each column shows the zoomed-in recovered and error images for different techniques. Each technique is identified by the text below the recovered images and its performance is reported as pairs (EOF, SSIM) below the corresponding error image.

2.3. Problem Formulation

Using the tagging MR encoding formulation improvement in MRI speeds will be achieved by acquiring fewer number of tag encode lines than the number of phase encode lines suggested by the Nyquist sampling theorem. To recover an MR image from under-sampled data, the following problem is solved:

$$\min_{\rho} \; f(\rho) \;\; s.t. \; \frac{1}{2} \| \, d_{tag} - \mathbf{E}\rho \, \|_2 \leq \epsilon \tag{7}$$

where, ϵ^2 is the estimated upper bound on the noise power and $f(\rho) = \| \, \Gamma \, \|_1$, Γ is the composite representation of all patches of image ρ in the redundancy encoding dictionary $\mathbf{G}$ as described in (6). Note in section 3, experiments are also performed with replacing the redundancy encoding by wavelet transform, for which $f(\rho) = \| \, \Psi^* \rho \, \|_1$, where Ψ is a wavelet basis. The solution to (7) for all experimental results presented in this paper are obtained using the the NESTA toolbox which implements the Nesterov's algorithm [12]. Few minor modifications were performed to handle complex images.

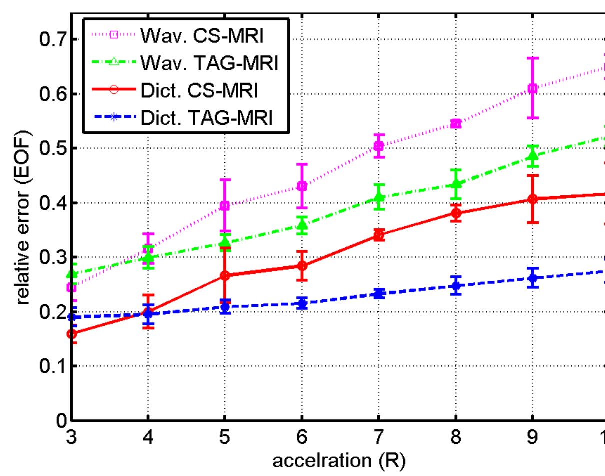

Fig. 2: ($\mu \pm \sigma$) Relative error (EOF) vs. accelerations (R) curve for different MR image recovery methods on the in-vivo myocardial perfusion dataset.

3. EXPERIMENTS AND RESULTS

The proposed fast dynamic MRI technique is experimentally validated using an in-vivo myocardial perfusion dataset. The perfusion data was acquired on a 3T Siemens scanner with a saturation-recovery sequence and comprises of an image matrix of size 90x190x70 (phase-encodes x frequency encodes x temporal slices). To evaluate the quality of recovered images following metrics are used: (1) EOF : relative error and, (2) SSIM: structural similarity index. The relative error (EOF) is calculated as $\frac{\|\rho - \rho^*\|_2}{\|\rho\|_2}$, where ρ is the reference image and ρ^* is the recovered image. SSIM provides a measure to assess the degradation of structural information, it compares local pixel-intensity patterns that are normalized for luminance and contrast [13].

To separate the benefits of the tagging based MR signal encoding from those of redundancy encoding using learned dictionaries, multiple experiments are run and reported for. The experiments are simply permutations of two acquisition schemes (sensing basis) and the two selected sparsifying bases. The tagging based MR signal encoding is compared with the variable density under-sampled Fourier encoding scheme and for convenience, hereafter these are identified by the *TAG-MRI* and the *CS-MRI* abbreviations, respectively. Similarly, the wavelet basis is selected for comparison with the patch-based redundancy encoding sparsifying basis and these will be identified by the *Wav.* and *Dict.* abbreviations, respectively. Thus, *Wav. CS-MRI* corresponds to the seminal compressed sensing approach of [4], *Dict. CS-MRI* is closer to the approach of [7] and, *Dict. TAG-MRI* corresponds to the proposed approach detailed in section 2.

For all *TAG-MRI* experiments, SPAMM sequences capable of creating sinusoidal spatial modulations in two separate-directions are simulated. Each SPAMM simulated sequence is parameterized using 4 variables, namely: 1) the two sinusoidal periodicities $T_{m,1}$ and $T_{m,2}$, and 2) the two directions of modulation axis, $v_{m,1}$ and $v_{m,2}$. Specifically, the spatial modulations are simulated as:

$$w_m(r) = \left|\cos \frac{2\pi}{T_{m,1}}\, r.v_{m,1}\right| * \left|\cos \frac{2\pi}{T_{m,2}}\, r.v_{m,2}\right| \qquad (8)$$

For all experiments, the four parameters are randomly selected from uniform distributions over the following intervals: 1) $T_{m,i=1,2} \in [2\ \ 32]$, 2) $\angle(v_{m,1}, x) \in [-\pi/4\ \ \pi/4]$ and, 3) $\angle(v_{m,1}, v_{m,2}) \in [\pi/18\ \ 4\pi/9]$. For all *Dict.* experiments, a patch-based dictionary $\mathbf{G}$ with 256 atoms is trained for 4x4 patches with a sparsity of $T_0 = 5$. To train the dictionary $\mathbf{G}$, 2 fully referenced images are randomly selected from the temporal slices and removed from the test data.

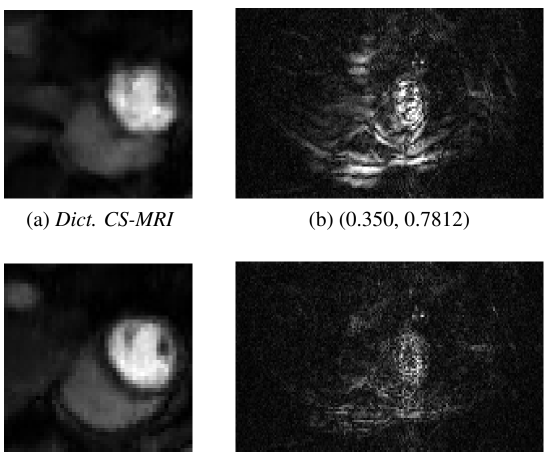
(a) *Dict. CS-MRI* (b) (0.350, 0.7812)
(c) *Dict. TAG-MRI* (d) (0.228, 0.8402)

Fig. 3: Zoomed-in recovered and complete error images for the *Dict. CS-MRI* & *Dict. TAG-MRI* techniques at acceleration R = 8.

Fig. 1 shows the recovered and the corresponding error images for a temporal slice at the acceleration factor of R = 4 for all the experiments. For better visualization of recovered characteristics, only the zoomed regions of recovered and error images are shown. The error images have been scaled identically. Fig. 2 characterizes the performance of all the techniques as a function of acceleration (R) in terms of the EOF. From Fig. 1 and Fig. 2, the following conclusions can be made. Firstly, the redundancy encoding using the patch-based dictionary outperforms the wavelet sparsifying basis for both the data acquisition methods. Secondly, for a fixed sparsifying basis, the TAG-MRI sampling method outperforms the standard under-sampled Fourier sampling method of CS-MRI at all accelerations $\geq$ 4. The marginally lower performance of the TAG-MRI compared to the CS-MRI at R=3 can be attributed to the following two reasons: 1) most of the k-space energy resides in its central region, thus a Gaussian profile based variable density sampling suffices to capture most of the energy and, 2) the TAG-MRI encoding matrix $\mathbf{E}$ is ill-conditioned, this is due to the limitation in the number of discretized tagging profiles that can be simulated. Consequently, the conditioning of the matrix $\mathbf{E}$ improves with increasing acceleration factors. Thirdly, the proposed (*Dict. TAG-MRI*) outperforms all other techniques at high accelerations. This is due to the fact that each acquired sample in the TAG-MRI method is a mixture of the standard k-space samples, which leads to a more uniform coverage of the k-space information than the CS-MRI sampling scheme. Thus, the TAG-MRI method recovers the edges and fine-structures with better accuracy than the CS-MRI method at high accelerations. This observation is further emphasized in Fig. 3 which shows the zoomed recovered and complete error images for images recovered using the *Dict. CS-MRI* and the *Dict. TAG-MRI* methods at the high acceleration R = 8.

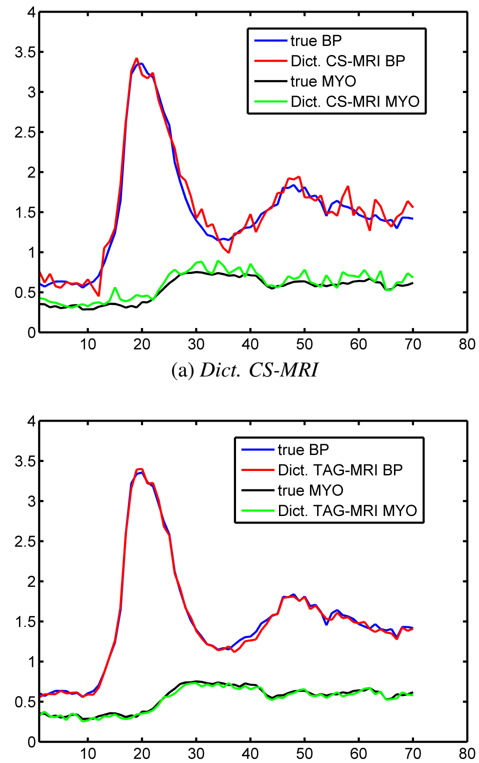

(a) *Dict. CS-MRI*
(b) *Dict. TAG-mRI*

Fig. 4: Time-series plot of averaged signal intensity for recovered (at R = 6) and reference images for the in-vivo myocardial perfusion dataset.

Fig. 4a and 4b compare the time-series plots of averaged signal intensity in selected blood pool and myocardium regions in reference images with that of the recovered images at acceleration R = 6 using the *Dict. CS-MRI* and the *Dict. TAG-MRI* techniques, respectively. The selected blood pool (in red) and myocardium (in green) regions are shown in Figs. 1a. As expected, the time series curve for recovered images using the TAG-MRI scheme follows the reference curve more closely than the curve for the CS-MRI sampling scheme.

4. CONCLUSIONS

This paper presents a novel MR signal encoding formulation using tagging radio frequency pulses. This new encoding formulation is further combined with dictionary learning techniques for sparse representations of signals to perform redundancy encoding for a dynamic MR image recovery problem. Preliminary results for dynamic MRI recovery experiments on an in-vivo cardiac dataset are better than the previously established fast dynamic MRI methods based on variable density k-space sampling.

5. REFERENCES

[1] M. Jerosch-Herold, R.T. Seethamraju, C.M. Swingen, N.M. Wilke, and A.E. Stillman, "Analysis of myocardial perfusion MRI," *Journal of Magnetic Resonance Imaging*, vol. 19, no. 6, pp. 758–770, 2004.

[2] B. Madore, G.H. Glover, and N.J. Pelc, "Unaliasing by Fourier-encoding the overlaps using the temporal dimension (UNFOLD), applied to cardiac imaging and fMRI," *Magnetic Resonance in Medicine*, vol. 42, no. 5, pp. 813–828, 1999.

[3] J. Tsao, B. Behnia, and A.G. Webb, "Unifying linear prior-information-driven methods for accelerated image acquisition," *Magnetic Resonance in Medicine*, vol. 46, no. 4, pp. 652–660, 2001.

[4] M. Lustig, D.L. Donoho, J.M. Santos, and J.M. Pauly, "Compressed Sensing MRI," *Signal Processing Magazine, IEEE*, vol. 25, no. 2, pp. 72 –82, 2008.

[5] C. A. Mistretta, O. Wieben, J. Velikina, W. Block, J. Perry, Y. Wu, K. Johnson, and Y. Wu, "Highly constrained backprojection for time-resolved MRI," *Magnetic Resonance in Medicine*, vol. 55, no. 1, pp. 30–40, 2006.

[6] L. Ge, A. Kino, M. Griswold, C.A. Mistretta, J.C. Carr, and D. Li, "Myocardial perfusion MRI with sliding-window conjugate-gradient HYPR," *Magnetic Resonance in Medicine*, vol. 62, no. 4, pp. 835–839, 2009.

[7] V. Singh and A.H. Tewfik, "Redundancy Encoding in Dynamic MR Imaging using Structured Sparsity," in *MICCAI Wshp. Sparsity Techniques in Medical Imaging*, 2012, pp. 1–8.

[8] L. Axel and L. Dougherty, "MR imaging of motion with spatial modulation of magnetization," *Radiology*, vol. 171, no. 3, pp. 841–845, June 1989, PMID: 2717762.

[9] E. Ibrahim, "Myocardial tagging by Cardiovascular Magnetic Resonance: evolution of techniquespulse sequences, analysis algorithms, and applications," *Journal of Cardiovascular Magnetic Resonance*, vol. 13, no. 1, pp. 1–40, 2011.

[10] J.P. Haldar, D. Hernando, and Zhi-Pei Liang, "Compressed-sensing MRI with random encoding," *Medical Imaging, IEEE Transactions on*, vol. 30, no. 4, pp. 893 –903, Apr 2011.

[11] M. Aharon, M. Elad, and A. Bruckstein, "K-SVD: An Algorithm for Designing Overcomplete Dictionaries for Sparse Representation," *Signal Processing, IEEE Transactions on*, vol. 54, no. 11, pp. 4311–4322, 2006.

[12] S. Becker, J. Bobin, and E. J. Cands, "NESTA: a fast and accurate first-order method for sparse recovery," *SIAM Journal on Imaging Sciences*, vol. 4, no. 1, pp. 139, 2011.

[13] Z. Wang, A.C. Bovik, H.R. Sheikh, and E.P. Simoncelli, "Image quality assessment: from error visibility to structural similarity," *Image Processing, IEEE Transactions on*, vol. 13, no. 4, pp. 600 –612, april 2004.